

24D Onshore CCS Seismic MMV Experiment

Lee Hunt, Carbon Alpha

Eric Street, Carbon Alpha

Graham Hack, Carbon Alpha

Jason Schweigert, BJV Design Inc.

Matthew Allen, BJV Design Inc.

Summary

This presentation is a direct sequel to another presentation at this convention, titled “24D Onshore CCS Seismic MMV Tactic,” and completes the workplan laid out in that paper. Both 24D presentations are companions to an overarching carbon capture and permanent underground storage (CCS) strategy called Theseus, which is also presented at this convention in the talk titled, “Theseus Onshore CCS Seismic MMV Strategy.”

For context, the Theseus strategy is concerned with lowering the capital costs and environmental disturbance caused by the seismic elements of MMV in onshore CCS projects. The 24D aspect of Theseus involves minimizing the amount of repeat 3D surveys in MMV in favor of a small number of repeat 2D seismic lines. In the previous 24D paper, we described how 24D requires a 3D design in which 2D lines can be extracted—anywhere within the 3D survey—to serve as a baseline against future repeat 2D lines. The baseline 3D survey must also serve in its multifaceted role as a 3D, where it must address the characterization of the storage reservoir and seal section. The central problem with 24D is to determine the best 3D design to achieve both needs—baseline 3D and repeat 2D—with high quality and capital efficiency. In the example given in that paper, capital costs were theoretically reduced by up to 57%, and surface disturbances at closure time were reduced by as much as 96%.

In this presentation, we show the results of a full 3D raytracing and processing experiment to produce the 3D survey most appropriate for 24D. This experiment will demonstrate how the theoretical benefits discussed in the earlier presentations could be achieved.

Theory

Please refer to the companion papers on 24D and Theseus for background theory on seismic MMV.

The potential advantage of 24D, from a cost and surface disturbance perspective, is that any 3D survey shot for MMV should contain or be able to produce 2D lines for baseline comparison to native repeat 2D surveys. There is a cost and scheduling advantage here because no explicit 2D baseline survey need ever be shot in the field. Greater advantage is gained if the repeat 2D lines replace the repeat 3D surveys. This proposition is only reasonable if any number of 2D lines, in any position within the baseline 3D, can be produced. Such flexibility is required because it cannot be unequivocally known how many 2D lines would be required for repeat 2D prior to shooting the baseline 3D. Reservoir characterization and reservoir and plume modelling aided by the baseline 3D should inform the repeat 2D requirements. As the CCS injection proceeds, there may also be reason to alter repeat seismic positioning, which places additional need on the baseline 3D to be able to produce 2D comparable baseline lines anywhere.

The repeat 2D problem is thus a problem in 3D design and processing.

Method

In the preceding “24D Onshore CCS Seismic MMV Tactic” paper we defined the concept of a master 3D survey, which contained a series of candidate sub-geometries. Our method now is to create a 3D subsurface model in which we then shoot a 3D ray-tracing experiment of the master survey and, equivalently, acquires the experimental data for each sub-geometry. A processing and interpretation exercise is then executed, the results of which evaluate each sub-geometry’s fitness for 24D.

The subsurface model design begins with a generic version of the Basal Cambrian Sand (BCS) storage reservoir and Cambrian Deadwood (DDWD) seal section. This storage complex was chosen because of its relevance to ongoing CCS activity in Alberta, Canada (Hunt et al., 2023). Figure 1 is a 1-dimensional representation of this storage complex.

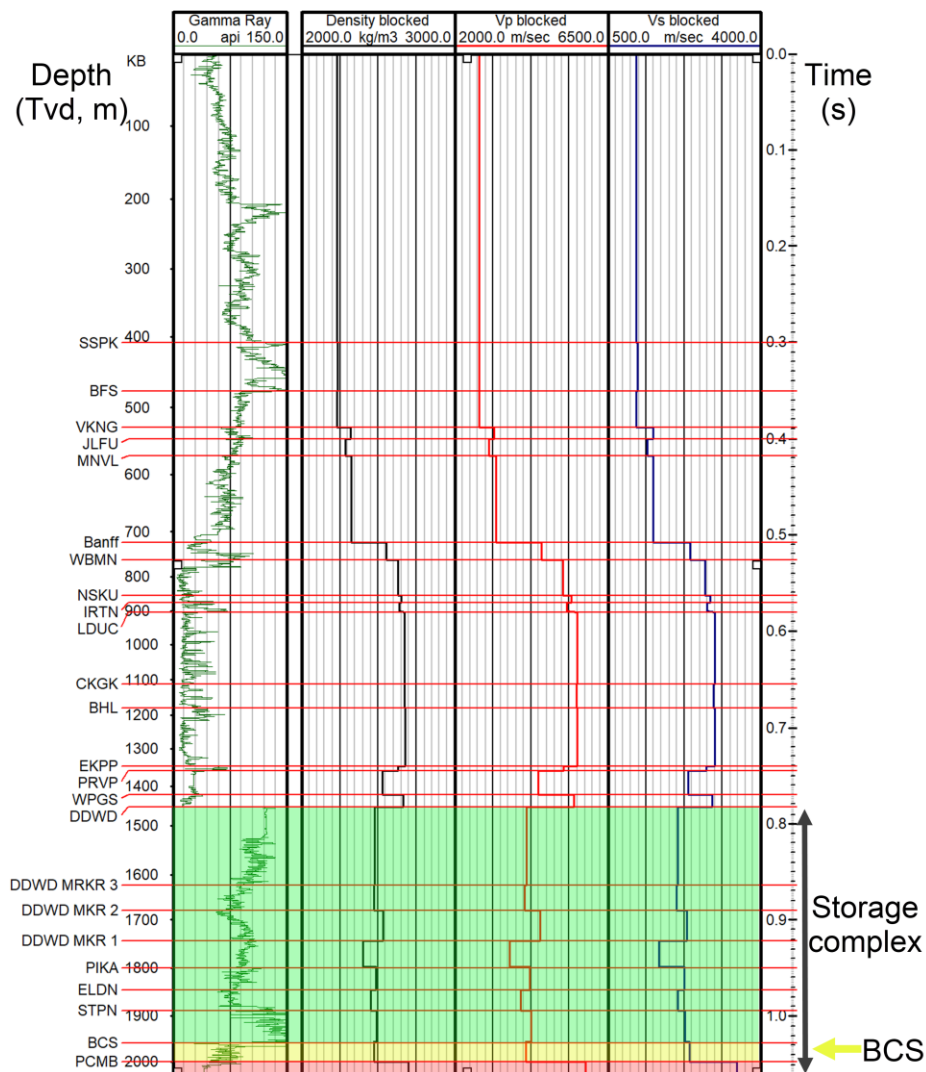


Figure 1; 1-dimensional representation of the subsurface model. The full 3-dimensional version of the subsurface model has added complexity in the form of a series of Precambrian highs.

The BCS storage reservoir is 40m thick, and its base, the Precambrian (PCMB), is at 2000m depth.

The model is flooded in 3-dimensions with these blocked layers, and a series of Precambrian highs (monadnocks) are added. There are 6 monadnocks in total. Each is perfectly square, oriented in the north-south and east-west directions. Their dimensions are: 50m x 50m, 100m x 100m, 200m x 200m (there are two of these), 300m x 300m and 500m x 500m. All the monadnocks are 30m in height, except for the 500m x 500m monadnock, which is 60m in height. The monadnocks are steeply built and have a 60-degree angle to the horizontal. The monadnocks are essential to the model experiment as they become an objective imaging challenge for both the model 3D survey and the 2D lines. Before we illustrate the positions of these monadnocks within the full 3-dimensional subsurface model, it is helpful to define the shooting geometries for the ray tracing experiment that will be conducted.

The master geometry is depicted in Figure 2, with the two native 2D lines shown in blue shading. Normally, we would not shoot separate baseline “native” 2D lines, but we have done so here to control our experiment. The master geometry contains north-south and east-west lines, each spaced 350m apart. Both sources and receivers are placed on these lines, each of which have a 50m interval. The native 2D lines have a 25m receiver interval and a 50m source interval. The native 2D lines were chosen so that Line 1 is parallel to the north-south lines in the master geometry, but offset from directly hitting those lines, and Line 2 runs at an oblique angle through the master geometry.

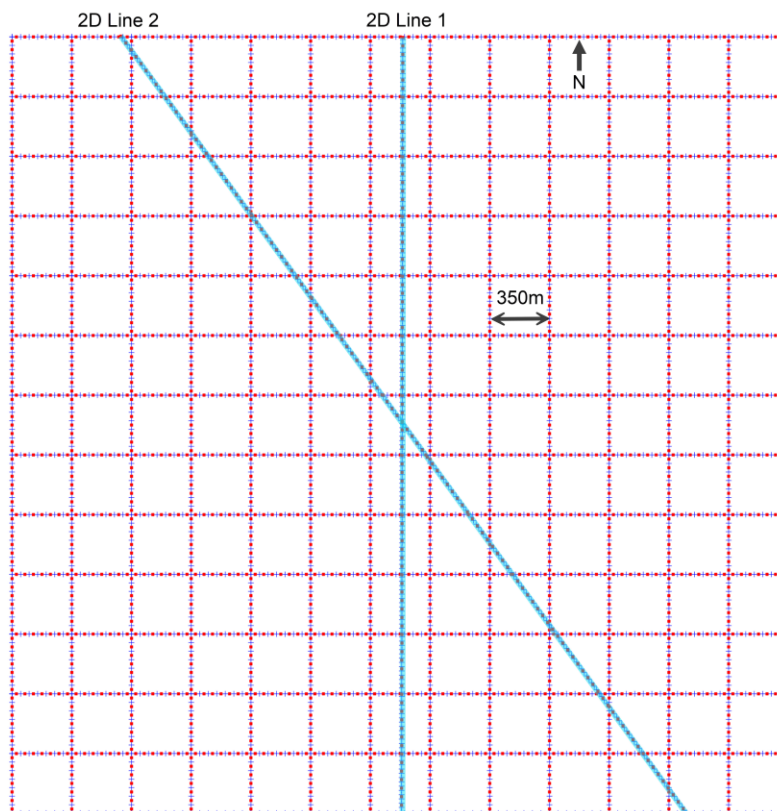


Figure 2; Master 3D layout with native 2D lines shown in blue shading. Red circles depict shots and blue crosses depict receivers.

This master geometry can be broken into numerous sub-geometries. Figure 3 illustrates the 4 sub-geometries examined in this experiment. They are, in respective order, (a) an orthogonal geometry, (b) a parallel geometry, (c) a zig-zag geometry and (d) a geometry created for this experiment that we term reverse zig-zag. The parallel geometry has too broad of a line spacing to be termed a Mega-Bin survey (Goodway and Ragan, 1996).

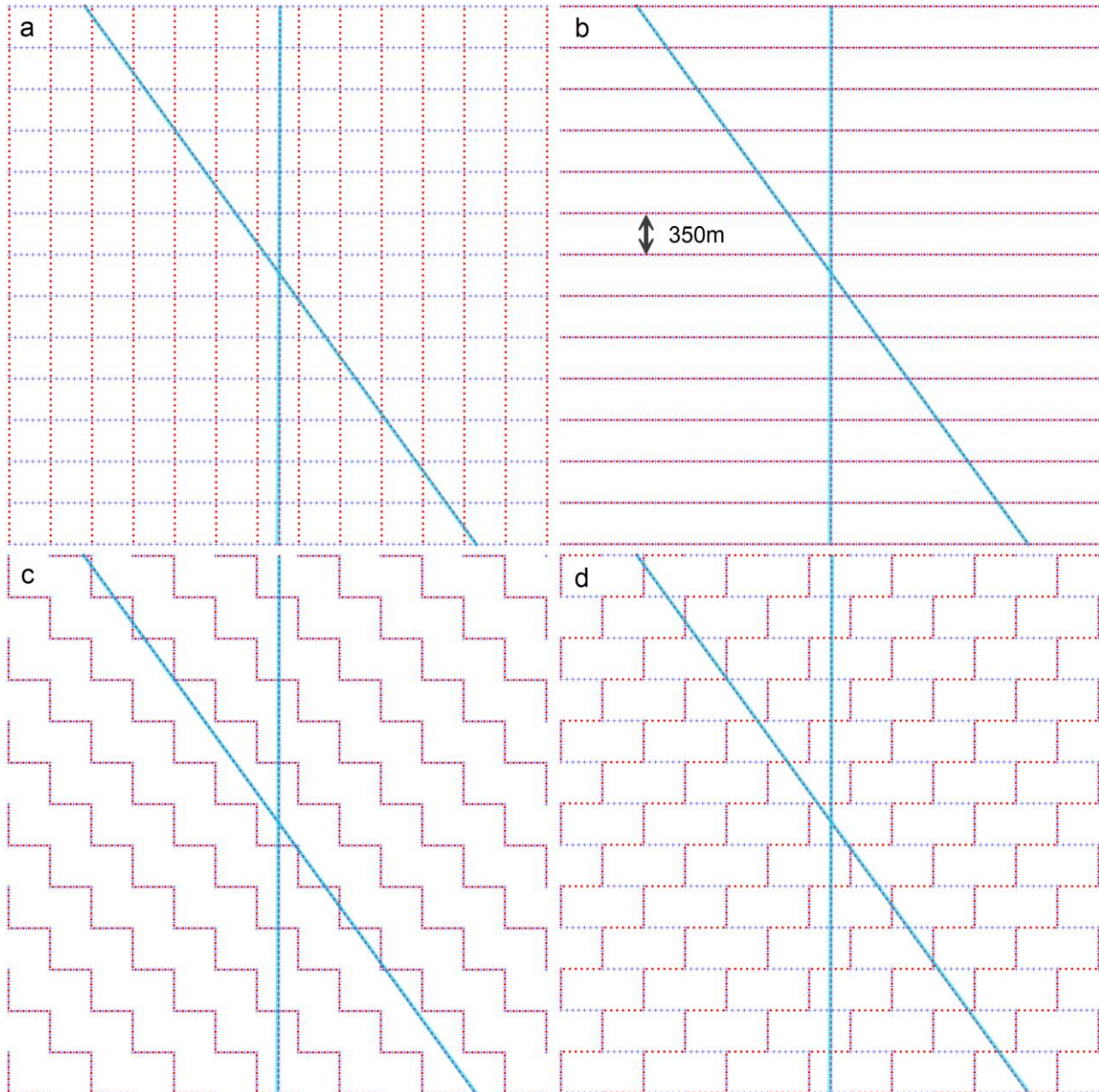


Figure 3; Four sub-geometries that can be created from the master geometry. The native 2D lines are illustrated with blue shading. Red circles depict shots and blue crosses depict receivers. (a) depicts an orthogonal geometry, (b) depicts a parallel geometry, (c) depicts a zig-zag geometry, and (d) depicts a hybrid zig-zag geometry, which we call a reverse zig-zag.

The subsurface model is illustrated with respect to the master geometry and native 2D lines in Figure 4, which also shows a time map of the Precambrian surface. The non-structured surface of the Precambrian is at approximately 1034ms and is cut-off in this image so that the seismic geometries can be seen. Because of this choice, the monadnocks are the only geologic features visible in the figure. The 2D lines intersect all but 2 of the monadnocks, and Line 2 just misses intersecting the largest of these Precambrian highs.

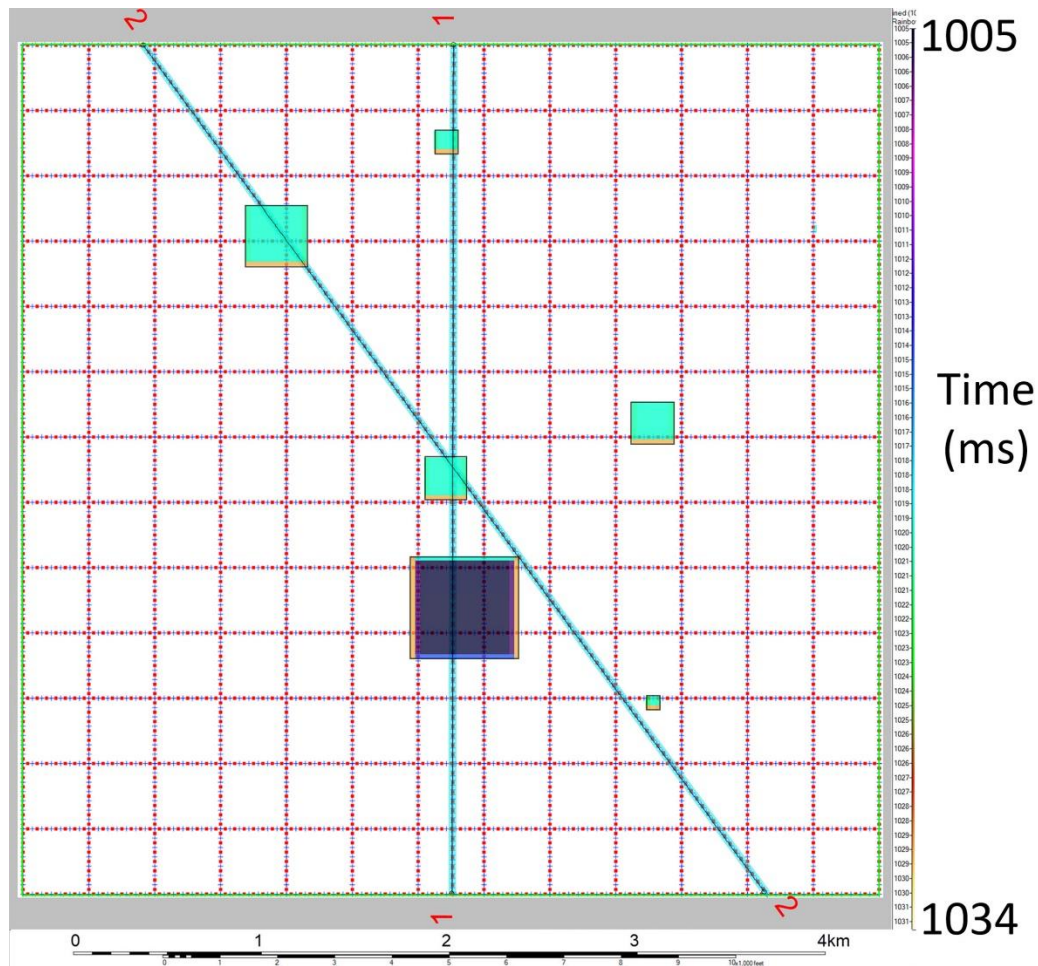


Figure 4; Time map of the Precambrian surface, illustrating the positions of the 6 monadnocks relative to the master 3D geometry and the native 2D lines (in blue shading). The non-structured Precambrian surface is at 1034ms, and is cut off from being colored so that the geometry and highs can be clearly seen.

The 2D and 3D ray tracing was conducted on this model using the travel-time method described in Chapman (2004). Reflectivities were defined by the 1-dimensional model layer properties and were normal incidence (no AVO). The master 3D was synthetically shot, followed by each sub-geometry (equivalent to decimating the synthetic shoot of the master), and then the native 2D lines were synthetically shot.

All 3D volumes were processed, including 5D interpolation (Stanton, 2021) and 3D migration. To create the 24D reconstructed 2D lines, each 3D volume was also interpolated into the 2D geometries of Line 1 and Line 2. These 5D reconstructed lines were then 2D migrated. The native 2D lines were separately processed and 2D migrated. The experiment was repeated for a version of each of the 3D surveys where the shot interval was increased for all geometries from 50m to 100m.

The evaluation of which 3D geometry produces the best reconstructed 2D lines for time lapse analysis was conducted using both qualitative and quantitative means. Qualitative comparisons were made between each reconstructed line and the native 2D lines. This is the key comparison required to evaluate fitness for time-lapse analysis. Another qualitative comparison was made between each reconstructed line and an extraction from the 3D volume along the transect of the 2D lines. To be clear, this first comparison is between 2D migrated data, and the second is between a either a native 2D line or a 5D reconstructed line given a 2D migration and a fully 3D migrated line along the same transect. The second comparison therefore evaluates 2D versus 3D imaging. Quantitative analysis for each of these comparisons is then carried out by calculating the correlation coefficients produced by comparing the amplitudes along the Precambrian surface between native 2D lines and reconstructed lines, and all the 2D lines and 3D transect. Further quantitative analysis was performed on difference stacks between the native 2D lines and the reconstructed lines.

The evaluation of the 3D geometries in their role as a 3D survey was carried out qualitatively comparing the mapping of the monadnocks, and quantitatively by correlating the amplitudes for the Precambrian surface between the geometries. The highly sampled master geometry was used as the reference for these correlative measures on the 3D sub-geometries.

Results

We will only present a selection of the results in this abstract. Comprehensive images for both lines, map images and correlation coefficients will be shown in the presentation.

Figure 5 shows the 3D transect along Line 2, as produced from the master geometry. It represents a reasonable representation of the correct answer—though from a 3D imaging, correct subsurface perspective rather than from the perspective of 24D. The reason for this distinction is that one of our two key objectives is to produce reconstructed 2D lines for comparison to native 2D lines. So, there is the correct geological answer, and the correct answer from a time-lapse perspective. If the two answers are quite different we may have cause for concern, however we argue that an analysis of this issue may be conducted on the baseline 3D, prior to shooting native 2D lines. Such experimentation could potentially reposition the planned-for 2D lines to minimize 3D imaging problems.

The 3D-imaged 3D transect does a good job of imaging the two monadnocks that Line 2 intersects. The near miss of the large 500m x 500m monadnock is also well imaged. The 200m x 200m monadnock is reasonably well imaged on its top, but not perfectly imaged at the base. Overall, the features are very well-imaged.

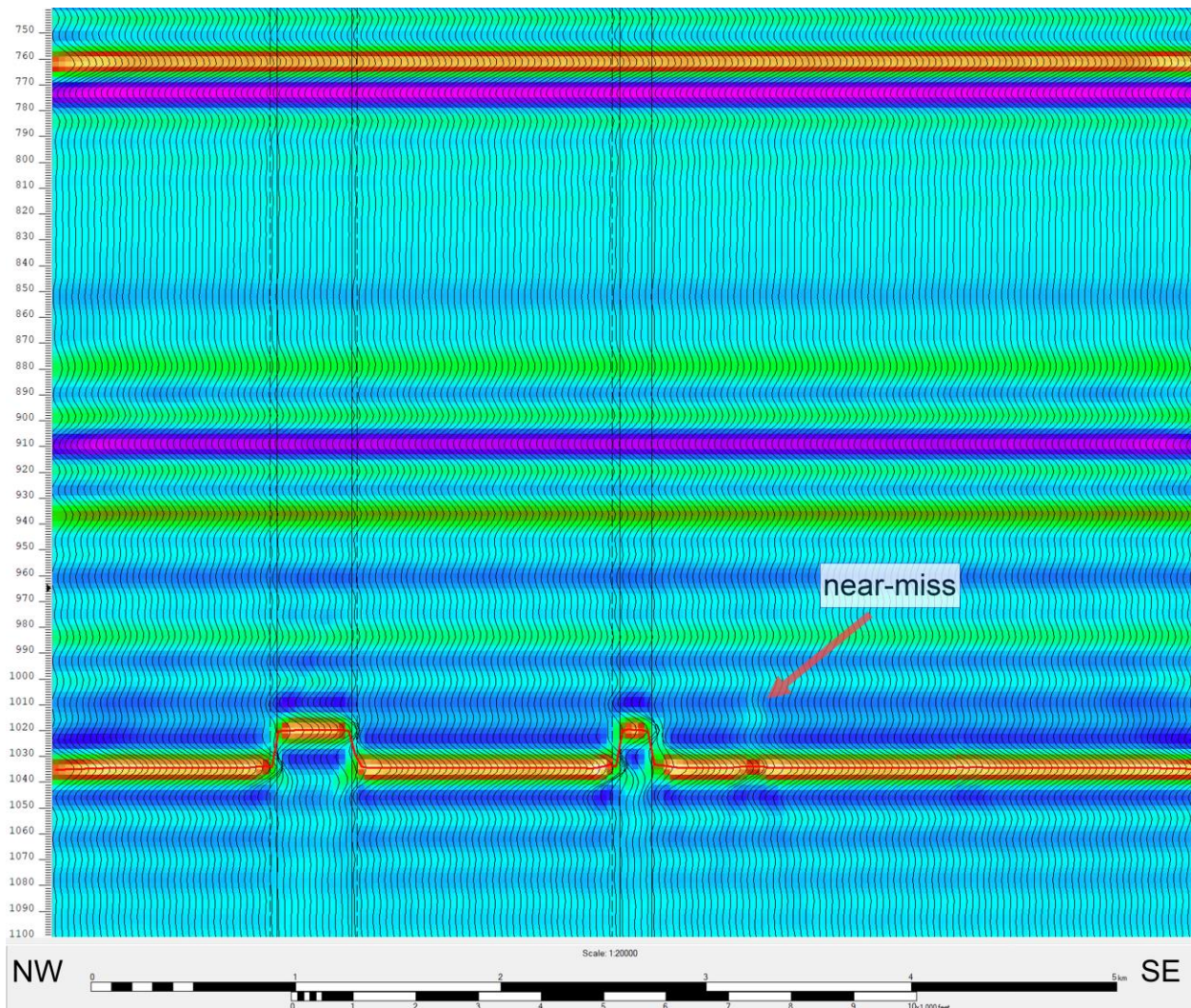


Figure 5; The 3D transect along Line 2 from the master 3D geometry. The edges of the monadnocks are bounded by light vertical lines down the image.

Figure 6 shows the native 2D Line 2. While being very similar to the 3D transect shown previously, there are several important differences. The top of the two monadnocks are reasonably well imaged, but the bases of the monadnocks are not as sharply imaged as in the 3D transect. The area proximal to the near miss with the 500m x 500m monadnock is miss-imaged. This is a sideswipe effect and is interesting because it illustrates an important limitation of 2D imaging. Going back to our discussion on the “right” answer, this is a right answer for time-lapse imaging that is also partly wrong. The superiority—or relative correctness—of the 3D transect from Figure 5 to the native 2D line of Figure 6 is a clear example of the value of 3D imaging.

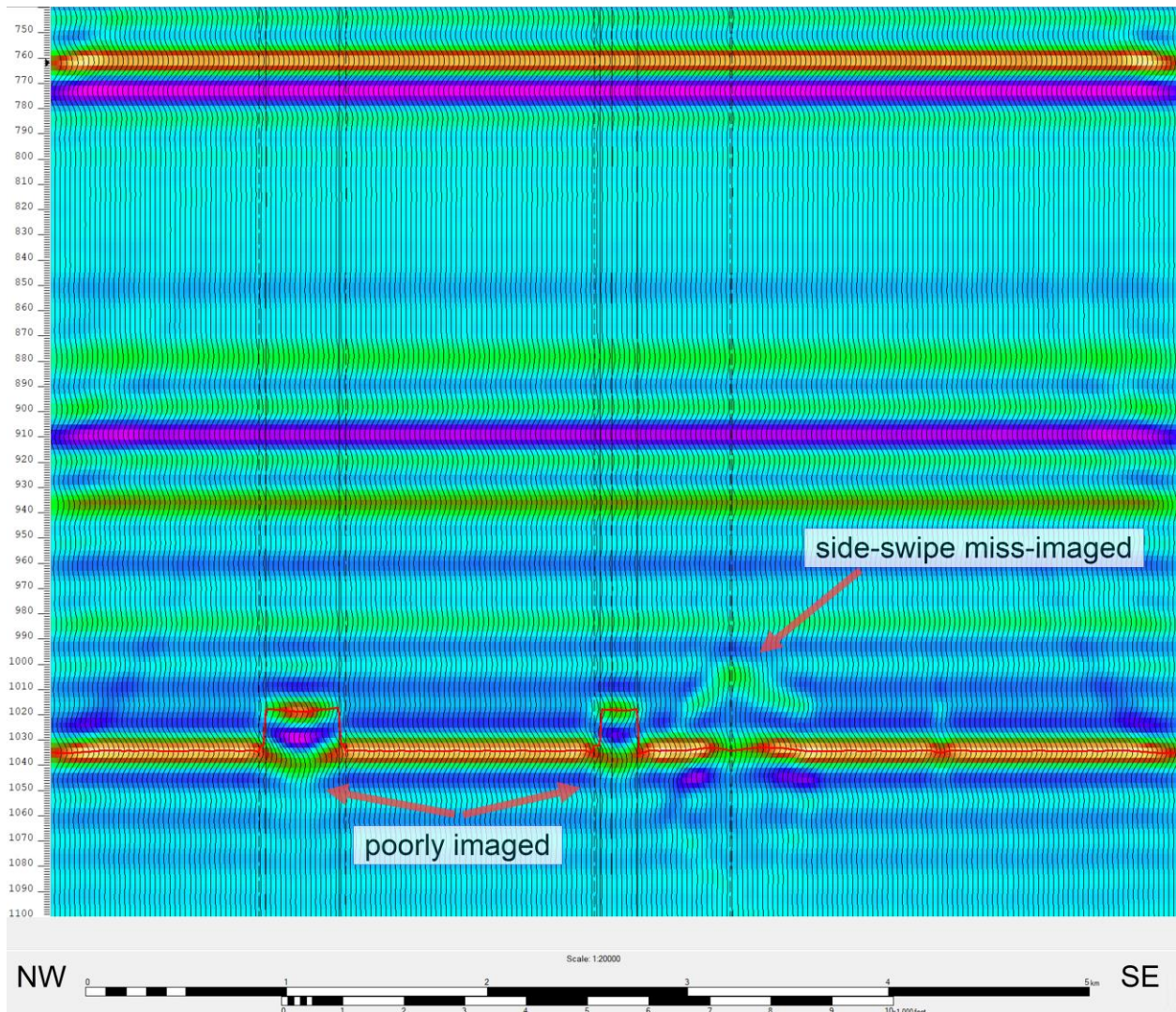


Figure 6; The native Line 2. The edges of the monadnocks are bounded by light vertical lines down the image. The intersection with Line 1 is also indicated near the middle of the 200m x 200m monadnock. The top of the two monadnocks that this line crosses are reasonably well imaged, although there are imaging errors at their base. The near miss of the 500m x 500m monadnock is miss-imaged on this line.

Figure 7 shows the reconstruction of Line 2 from the orthogonal sub-geometry. It is very similar in appearance to the native 2D line—meaning that it seems to be appropriate for time-lapse analysis. The Precambrian pick amplitudes between the reconstructions from the orthogonal geometry and the native 2D for both Line 1 and Line 2 give a correlation coefficient of 0.980, which is very high and is satisfactory for time-lapse. While it compares well to the native 2D line, this reconstruction also differs from the 3D transect in the same way that the native 2D line does. The bases of the monadnocks are poorly imaged, and the sideswipe effect from the 500m x 500m monadnock is evident. This is a remarkably useful result because it supports the argument that

we can accurately pre-diagnose potential 2D imaging issues with our 3D surveys and reconstruction method.

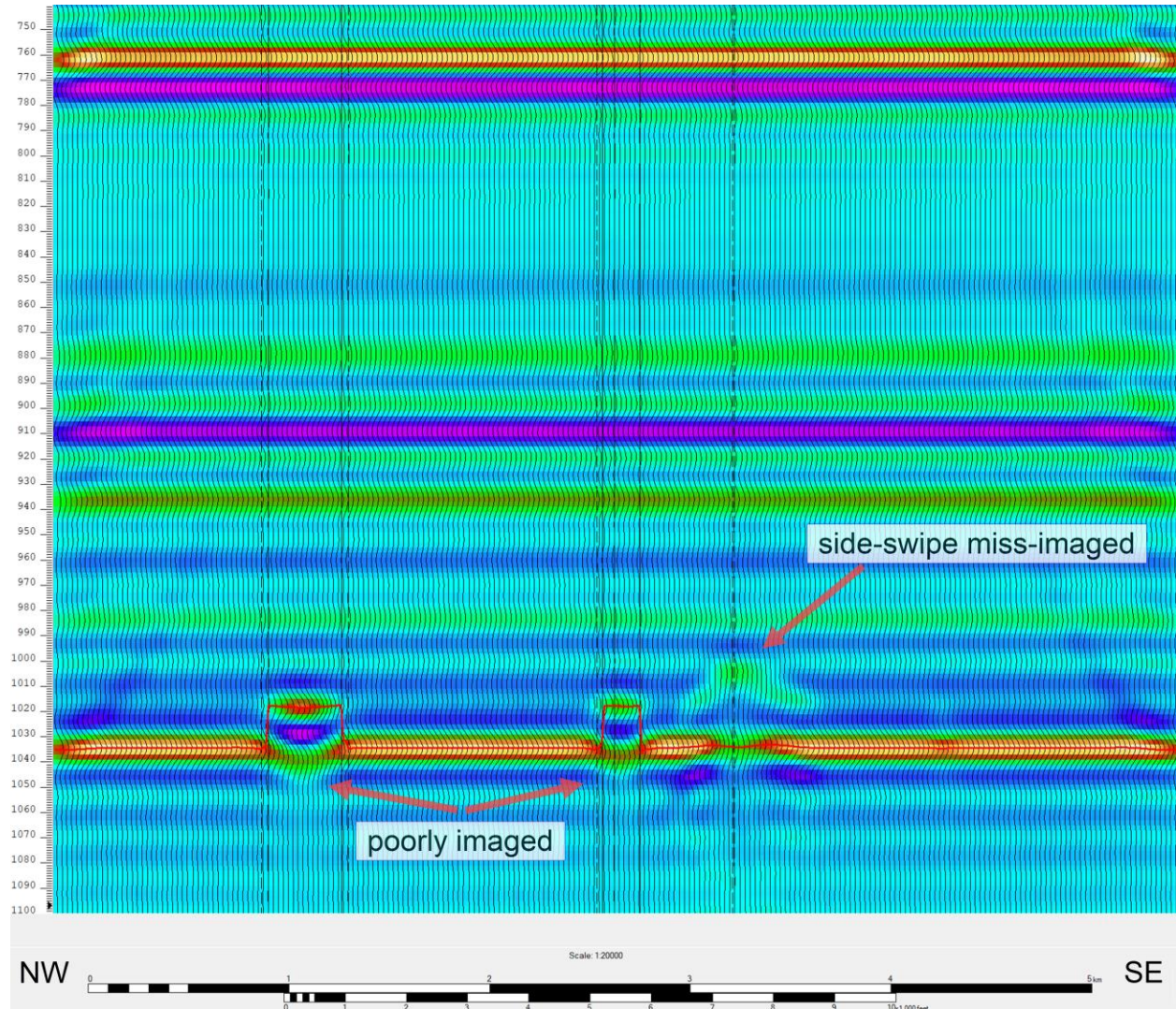


Figure 7; The orthogonal 2D reconstruction of Line 2. The edges of the monadnocks are bounded by light vertical lines down the image. The intersection with Line 1 is also indicated. The monadnocks are imaged almost as well—and very similarly—to how they were imaged on the native 2D line. The near miss of the 500m x 500m monadnock is miss-imaged on this line.

Figure 8 shows the reconstruction of Line 2 from the parallel sub-geometry. It is not very similar in appearance to the native 2D line—meaning that it seems to be inappropriate for time-lapse analysis. The Precambrian pick amplitudes between the reconstructions from the parallel geometry and the native 2D for both Line 1 and Line 2 give a correlation coefficient of 0.878, which is insufficient for time-lapse. The amplitudes of the top and base of the monadnocks are incorrect and the sideswipe is so poorly imaged that an interpreter may not identify it for what it

is. There is also ubiquitous noise in the image that was absent from the other images along Line 2.

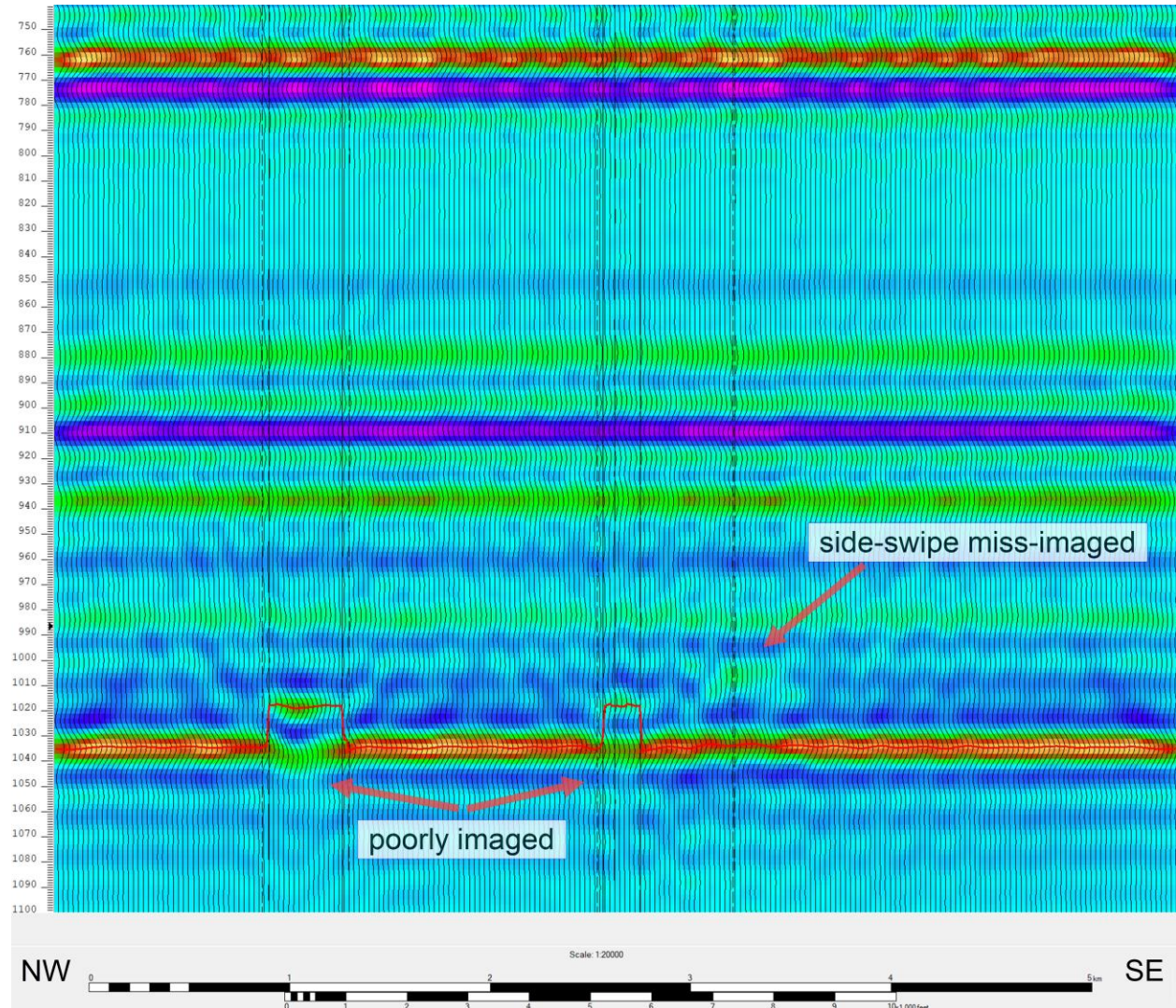


Figure 8; The parallel reconstruction of Line 2. The edges of the monadnocks are bounded by light vertical lines down the image. The intersection with Line 1 is also indicated. The top and base of the two monadnocks that this line crosses are poorly imaged. The near miss of the 500m x 500m monadnock is miss-imaged on this line.

The full presentation will show additional results and leads to a ranking of the sub-geometries for the purposes of 24D, within the context of this experiment. That ranking follows:

1. Orthogonal
2. Reverse zig-zag
3. Zig-zag
4. Parallel

The first three geometries yielded very similar, high quality, results that suggested that they may each be appropriate for the reconstruction of time-lapse quality 2D lines. In a real project, this assessment would depend on the particulars of the area, the data quality and noise characteristics, and the storage complex being considered.

It should be noted that this experiment was carried out with a particular set of rules, as defined in the companion paper, “24D Onshore CCS Seismic MMV Tactic.” Those rules required that all sub-geometries contain the same total number of sources and receivers and the same line spacings. While this is reasonable from the perspective of the experiment, it could be argued that it is unfair to any linear geometry such as parallel and zig-zag. The reason for unfairness comes from the fact that the parallel geometries involve less line cutting and typically involve tighter line spacings (Duncan et al., 2014). While we would opine that the parallel design is unlikely to compete well with the other (orthogonal-basis) geometries given a slightly tighter line spacing, the zig-zag geometry does compete very nearly as well even with the current line spacing and could potentially be superior with a slight reduction in spacing.

Feasibility and the unexpected

While the Theseus 24D MMV strategy proposes a series of ways in which both capital and environmental disturbances may be minimized, actual MMV plans arising from this philosophy must ensure that the goals of MMV are satisfied. MMV must assure both containment and conformance of the injected CO₂. The MMV scenario discussed in this paper and in the “24D Onshore CCS Seismic MMV Tactic” paper consider the possibility of a no-repeat 3D plan. Such an approach will not always be appropriate or feasible, for a variety of reasons. But even if we have reason to believe that the Theseus approach is applicable, such a no-repeat 3D version of Theseus must have a built-in provision to change if the unexpected were to occur. Figure 9 cartoons such a provision. The figure shows the MMV plan proceeding in time from left to right, in each time increment from the baseline 3D at time index 0 to the closure survey at time index 6. The modeled plume growth (Cinar et al., 2008, Nordbotten et al., 2005) is shown in purple and was used for the 2D and 3D MMV design. By repeat 2D survey #2, it is noted that the actual plume growth (in yellow) is elongated in the north-south direction and is departing significantly from the plume model. The departure from expectation triggers a revision in the survey, depicted by the arrows in the figure. We call this departure a trigger, in that it triggers a modification to the MMV plan. Depending on the severity and nature of the trigger, we might choose to make one of several modifications to the repeat survey taken at time index 3:

- 1) Additional 2D lines may be added to the 2D repeat survey.
- 2) A small 3D survey may be acquired instead of the repeat 2D survey.
- 3) A series of focused surveys (Brun et al., 2022) could be acquired rather than either a 2D or 3D repeat survey.

Depending on the results of this trigger-based survey, the repeats at subsequent timed indices will be altered. Figure 9 represents that two 2D lines are added (shown by red dashes) to the time index 3 survey, and additional lines are added to the 2D surveys at index 4, 5, and 6. This cartoon representation was inspired by a trigger-based discussion carried out in Furre et al. (2020).

Such flexibility is necessary for the Theseus 24D method to be adequate for the unexpected. The ability to produce additional baseline 2D surveys from the original baseline 3D through wavefield reconstruction is critical to this flexibility. The need to adapt to and mitigate the unexpected also confirms the value of the wavefield reconstruction approach over an approach that depends on presupposing with complete certainty what 2D lines might be needed later in the project life.

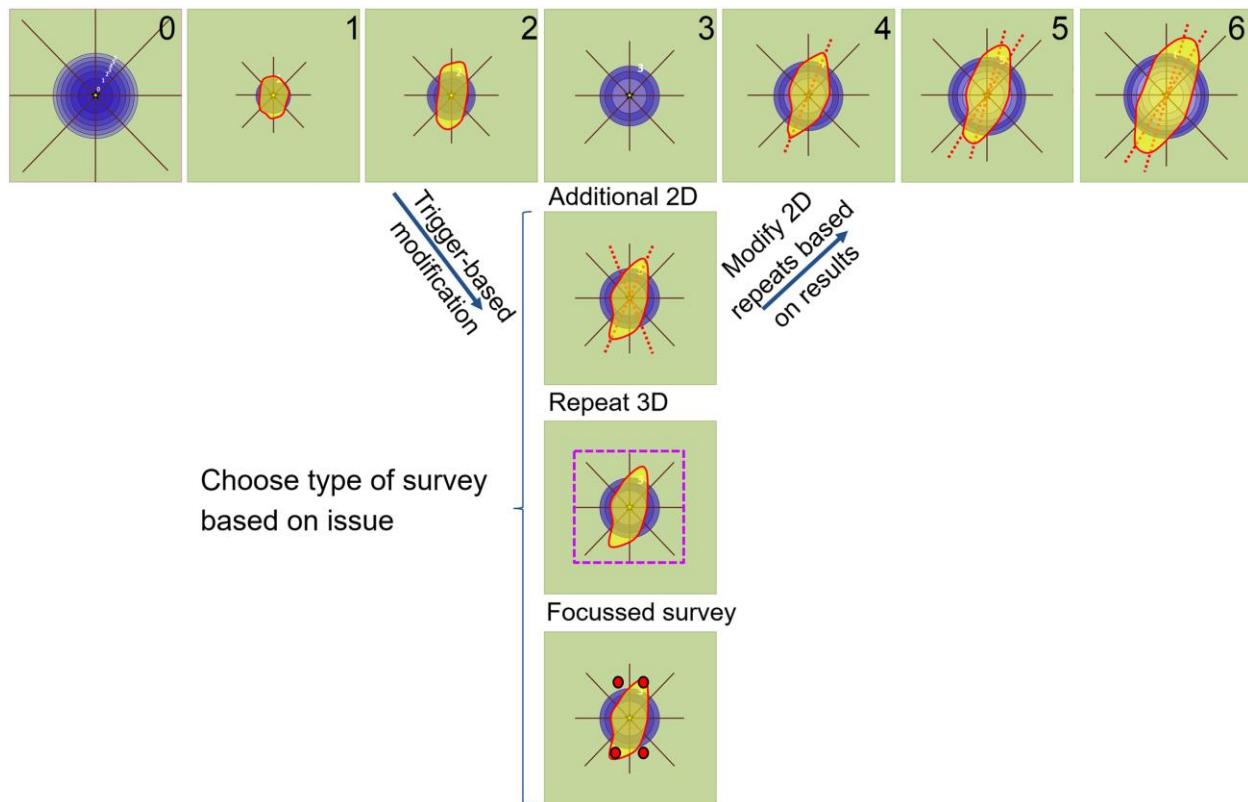


Figure 9; The Theseus 24D MMV plan must be flexible and change if there is a trigger anywhere in the MMV system. This example, inspired by Furre et al., 2020, cartoons potential modifications to the MMV plan if the plume (shown in yellow) departs in shape significantly from the model (shown in purple). The time index of the survey is shown in the upper right corner of each representation. Index 0 corresponds to the baseline 3D and closure plume model. The red dashed lines are additional 2D lines that are added to the MMV program following the identification of an unexpected plume asymmetry.

Conclusions

The experiment was executed, and the results were materially helpful in addressing the key requirements and questions of 24D.

The most impactful observation made from this work is that the 2D imaging of the monadnocks is materially inferior to the 3D imaging of them. These issues do not invalidate the 24D method, however, they are a warning that imaging effects need to be accounted for. This issue may be mitigated by experimenting on the baseline 3D to determine the positioning of the monitoring 2D lines where imaging issues will be minimized. Such a determination is practically achievable since the baseline survey is shot first, and the results of 24D processing experiments can be used to inform the repeat 2D positions. 2D versus 3D imaging effects should not be lightly dismissed, and this method does not do so—the experiment itself begins an exploration of these effects and could be taken further. On its own, this is a compelling example of 2D versus 3D imaging, and 2D sideswipe.

The experiment also illustrated that 5D interpolation to produce time-lapse appropriate 2D lines from a 3D survey is possible and can be achieved with numerous geometries. Some geometries were shown to be superior to others, though, with the parallel geometry being the worst performer within the constraints of the experiment. Reconstruction tests, as performed here on synthetic data, could also be applied to legacy 3D and 2D surveys to determine fitness of existing seismic for the 24D method.

Novel/Additive Information – legacy 3D test

This experiment is novel because it uses a synthetic 3D model to simulate a shoot and thus evaluate geometries for field service. This method could be used to test other seismic acquisition geometries cheaply prior to being used in the field. And this experiment revealed the best 3D geometries for the 24D concept. It also emphasized the value of 3D imaging over 2D imaging.

An unexpected outcome of this experiment is that it illustrates a processing test that could be used as the core element in a method to determine the fitness of legacy 3D surveys for baseline purposes in MMV for carbon storage projects. Legacy 3D is generally much cheaper than new shooting and can be immediately purchased without having to wait for a shooting season. This may be profoundly significant for some storage projects as it could materially lower seismic costs and reduce the scheduling impact of seismic.

Acknowledgements

We thank Aaron Stanton, Richard Bale and Eric Senetza of Key Seismic for their help on this project.

References

- Brun, V., J. De Sousa, E. Morgan, 2022, CO₂ injection detection using light time-lapse seismic monitoring, 83rd EAGE Annual Conference & Exhibition, 1-5, DOI: <https://doi.org/10.3997/2214-4609.202210275>
- Chapman, C., 2004, Fundamentals of Seismic Wave Propagation, Section 2.3, pp16-17, Cambridge University Press, <https://doi.org/10.1017/CBO9780511616877>
- Cinar, Yildiray, O. Bukhteeva, P. Neal, 2008, CO₂ storage in low permeability formations, 2008 SPE Improved Oil Recovery Symposium, SPE 114028
- Duncan, E., A. O'Byrne, and J Dalsin, 2014, Real vs. '5D' Data: An analysis of acquired vs. interpolated data in both the post-stack and the pre-stack domains for parallel and orthogonal geometries, CSEG Recorder, V 39, N 3.
- Furre, A.-K., R. Meneguolo, L. Pinturier, and K. Bakke, 2020, Planning deep subsurface CO₂ storage monitoring for the Norwegian full-scale CCS project: First Break, **38**, no 10, 55-60, doi: 10.3997/1365-2397.fb2020074
- Goodway, W., and B. Ragan, 1996, "Mega-Bin": Toward a cost effective "near symmetric patch geometry" for improved S/N & resolution for regular acquisition sampling and co-operative image processing"; CSEG Convention Abstracts p. 990-02.
- Grant, Timothy, and D. Morgan, 2018, Best Practices: CO₂ Storage Lecture – Carnegie Mellon University, Carbon Capture and Storage Short Course, 2/18, NETL-PUB-21697, OSTI 1547306
- Harvey, Stephen, J. Hopkins, H. Kuehl, S. O'Brien, and A. Mateeva, 2021, Quest CCS Facility: Time-Lapse Seismic Campaigns, 15th International Conference on Greenhouse Gas Control Technologies, GHGT-15, <http://dx.doi.org/10.2139/ssrn.3817070>
- Hunt, Lee, E. Street, and G. Hack, 2023, CCS expertise and analogic reasoning, CSEG Recorder, September, https://cseg.ca/wp-content/uploads/LHunt_CCS-Expertise-formatted-Aug22.pdf
- Nordbotten, Jan, M. Celia, S. Bachu, 2005, Injection and storage of CO₂ in deep saline aquifers: analytical solution for CO₂ plume evolution during injection, J. Transp Porous Med (2005) 58:339-360, DOI 10.1007/s11242-004-0670-9

Stanton, A., 2021, Sparse thresholding for regularization, interpolation and dealiasing, Society of Exploration Geophysicists Annual Meeting, p 2889-2893, DOI: 10.1190/segam2021-3584024.1

White, Don, K. Harris, L. Roach, M. Robertson, 2019, 7 years of 4D seismic monitoring at the Aquistore CO₂ Storage Site, Saskatchewan, Canada, SEG Technical Program Expanded Abstracts 2019, 4918-4922, DOI:10.1190/segam2019-3216776.1